AD-A128 908 HETERODYNE HOLOGRAPHY FOR VIBRATION ANSLYSIS(U) BROWN 1/1
BOVERI RESEARCH CENTER BADEN (SWITZERLAND)
B INEICHEN ET AL. AUG 80 F49620-79-C-0214

UNCLASSIFIED F/G 14/5 NL

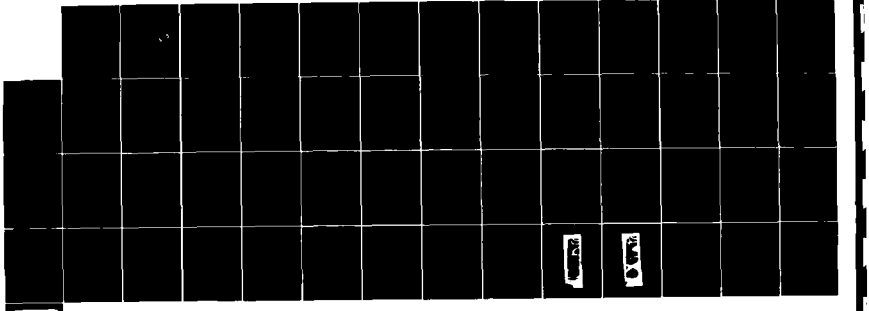

END
DATE FILMED
DTIC

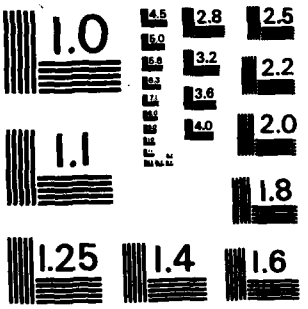

(1)

AD

HETERODYNE HOLOGRAPHY FOR VIBRATION ANALYSIS

FINAL TECHNICAL REPORT

BY

B. Ineichen, J. Mastner

AUGUST 1980

U.S. AIR FORCE EUROPEAN OFFICE OF AEROSPACE RESEARCH AND DEVELOPMENT

London, England

GRANT NUMBER F 49620-79-C-0214

Brown Boveri Research Center, CH-5405 Baden, Switzerland

REPORT DOCUMENTATION PAGE		READ INSTRUCTIONS BEFORE COMPLETING FORM
1. Report Number	2. Govt Accession No. AD-A126906	3. Recipient's Catalog Number
4. Title (and Subtitle) HETERODYNE HOLOGRAPHY FOR VIBRATION ANALYSIS		5. Type of Report & Period Covered FINAL TECHNICAL REPORT 01 Sep. 79 - 01 August 80 6. Performing Org. Report Number
7. Author(s) B. Ineichen, J. Mastner		8. Contract or Grant Number F 49620-79-C-0214
9. Performing Organization Name and Address BROWN BOVERI RSEARCH CENTER CH-5405 BADEN-DAETTWIL SWITZERLAND		10. Program Element, Project, Task Area & Work Unit Numbers PE - 61102F (AFWAL/FIBE) 62203F (AFWAL/POTP) Proj/Task/WU: 2034/N1/03 (AFWAL/FIBE), 3066/12/58 (AFWAL/POTP)
11. Controlling Office Name and Address AFWAL/POTP Wright-Patterson AFB, OH 45433		12. Report Date AUGUST 1980 13. Number of Pages
14. Monitoring Agency Name and Address EOARD/LNT Box 14 FPO New York 09510		15.
16. & 17. Distribution Statement Approved for public release; distribution unlimited.		
18. Supplementary Notes		
19. Key Words (U) SURFACE STRAIN: (U) STRAIN: (U) STRESS: (U) HOLOGRAPHIC: (U) INTERFERENCE: (U) HOLOGRAMS: (U) INTERFEROMETRY		

20. Abstract

The basic problems of quantitative determination of mechanical strain of vibrating object through holographic interferometry are discussed.

Time-average holography, which is most commonly used for holographic vibration analysis, can not be combined with heterodyne evaluation, since the interference fringes are already frozen in the hologram. Synchronized double-pulse holography can be employed in the same manner as pulsed double exposure holography. Moreover, real-time holography allows to investigate the temporal behaviour of vibrations, but only at one or a few points si-

JVC

FORM 1473

taneously, depending on the number of detectors employed. Both methods were tested.

The method uses essentially heterodyne holographic interferometry for the quantitative determination of the surface displacement from the fringe pattern in the image plane.

Finally, a nearly fully automated camera with photothermoplastic film is presented to achieve fast and dry in-situ recording and processing of holograms with high diffraction efficiency.

Summary

The basic problems of quantitative determination of mechanical strain of vibrating object through holographic interferometry are discussed.

Time-average holography, which is most commonly used for holographic vibration analysis, can not be combined with heterodyne evaluation, since the interference fringes are already frozen in the hologram. Synchronized double-pulse holography can be employed in the same manner as pulsed double exposure holography. Moreover, real-time holography allows to investigate the temporal behaviour of vibrations, but only at one or a few points simultaneously, depending on the number of detectors employed. Both methods were tested.

The method uses essentially heterodyne holographic interferometry for the quantitative determination of the surface displacement from the fringe pattern in the image plane.

Finally, a nearly fully automated camera with photothermoplastic film is presented to achieve fast and dry in-situ recording and processing of holograms with high diffraction efficiency.

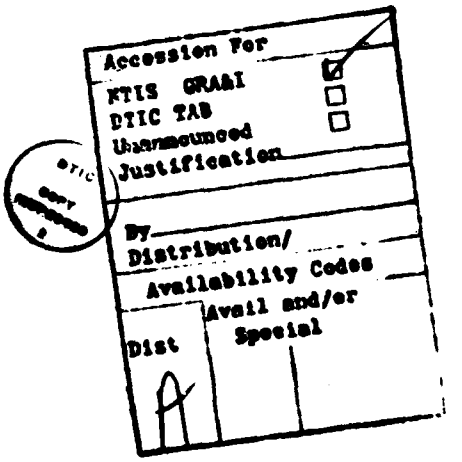

CONTENTS

LIST OF ILLUSTRATIONS

1. INTRODUCTION

Time-average holography is the common and convenient kind of holographic vibration analysis. However, quantitative information on the interference phase can only be obtained reliably from the maxima and minima of the interference fringes; any interpolation between fringes is difficult and not very accurate. Heterodyne holographic interferometry is an opto-electronic technique which overcomes this limitation and allows to determine the interference phase at any position within the fringe pattern with an accuracy of 1/1000 of a fringe (1).
To use the full potential of accuracy of heterodyne holographic interferometry it is necessary to store the information of the vibration amplitude holographically by some kind of double exposure recording and to perform the evaluation under stationary conditions afterwards. This can be accomplished by combination of stroboscopy and two-reference-beam holography.

2. HETERODYNE HOLOGRAPHIC INTERFEROMETRY

The basic idea of heterodyne interferometry is to introduce a small frequency shift between the optical frequencies of the two interfering light fields. This results in an intensity modulation at the beat frequency of the two light fields for any given point of the interference pattern. The optical phase

difference is converted into the phase of the beat frequency (2,3).

Two-reference beam holographic interferometry is applied in the following way to realize the heterodyne method for double exposure holographic interferometry, see Fig. 1. The first object state 01 is recorded using beam R1 as a reference. A stop is placed in beam R2 so that it does not illuminate the hologram plate which is a thermoplastic film. The second object state 02 is recorded in the same manner, except that beam R2 is used as a reference and beam R1 is stopped. All light fields during recording have the same optical frequency ωR. After processing the hologram is reconstructed with geometrically identical reference waves R1 and R2, but of slightly different optical frequencies $\omega 1$ and $\omega 2$, respectively. The reconstructed wave fields 01 and 02 have the same frequencies as their respective reference waves. This meets precisely the conditions necessary for heterodyne interferometry between these two reconstructed wavefields. The frequency difference $\Omega = \omega 1 - \omega 2$ has to be small enough to be resolved by photodetectors ($\Omega/2\pi < 100$ MHz). The relative 2×10^{-7} for visible light. The resulting changes in the propagation of the light waves are thus very much below any optical resolution.

Besides the standard holographic technique and equipment one needs for heterodyne holographic interferometry also methods to generate the desired frequency offset Ω, to detect the

modulated signals, and to measure their phase accurately (4,5).

The heterodyne technique can be applied, with some restriction, to nearly all known kinds of holographic interferometry. For this purpose it is only necessary that the two wavefields to be compared interferometrically can be reconstructed with slightly different optical frequencies. The heterodyne technique is not applicable to time-average holographic interferometry of vibrations, since the average wavefields show already frozen interference fringes in the hologram recording.

3. THERMOPLASTIC FILM CAMERA FOR HOLOGRAPHIC RECORDING

3.1 INTRODUCTION

Usually, an optical recording medium requires a certain processing to transform the recorded information into a form that is suitable for readout. In some applications, like Optical Memories (6), Optical Information processing (7) and Holographic Interferometry (8), this processing should be preferably done inside the recording configuration. In industrial applications, e.g. of the holography, the processing time should be as short as possible.

The conventional silver halide emulsions do not meet these requirements. Wet processing, consisting of wet chemical development and fixation, usually can not be accomplished in

the recording setup. A repositioning of the processed plate or film into the optical setup with an accuracy up to some fractions of the optical wavelength is very critical, and troublesome.

In the past two decades, this limited potentiality of conventional photographic materials has brought many investigators to explore the possibilities of new types of recording media. It was shown that the use of photothermoplastic materials for recording offers significant advantages due to the combination of the following properties of thermoplastic materials:

1. A considerably low value of the exposure energy is needed.
2. The diffraction efficiency is rather high.
3. The recording of information and processing for readout can be done in situ, so that no repositioning troubles are met.
4. If desired, the recorded information can be erased, and the material is then reusable for the next recording.

Experiments with a thermoplastic material on a glass carrier for information storage have started as early as 1959 (9). In the recent time a photothermoplastic film with a plastic carrier was developed, which is better suitable for industrial applications than the plate. Also cameras using the photothermoplastic film were introduced.

Nevertheless, some further optimization of this recording technique and the instrumentation are still necessary, to make them useful for high repetition rate laboratory experiments, for in-

dustrial applications and for difficult holographic recordings with large aperture.

3.2 PHOTOTHERMOPLASTIC FILM

The photothermoplastic film (e.g. Kalle PT-1000) consists of three layers (10). On the transparent plastic carrier a thin photoconductive layer is deposited, which is covered finally by a thin layer of the thermoplastic material.

For sensitizing the film, the surface of the thermoplastic materials is uniformly electrically charged. During the recording, the intensity distribution of the incident light produces a conductivity pattern in the photoconductive layer which results in a charge redistribution on the surface of the thermoplastic material. The surface-charge distribution produces finally a pattern of electrostatic forces in the thermoplastic material which is a replica of the light-intensity pattern to be recorded.

To develop the force pattern, the thermoplastic material has to be heated slightly above its melting point. Becoming soft, the surface is deformed under the influence of the electrostatic forces until at each point an equilibrium between the surface tension forces and the electrostatic forces is obtained. Being cooled down under the melting temperature, the thermoplastic material hardens again and the surface deformation becomes fixed. The surface of the developed film becomes slightly milky as if frosted.

To perform the phase transition of melting, a certain amount of heat must be delivered to the thermoplastic layer. This has to be done rather quickly to avoid surface charge loss due to conductivity of the thermoplastic material which rises drastically near the melting point. To obtain a fast softening, the material is heated for a short time far above the real melting temperature to pump the necessary develop heat into the thermoplastic layer in a very short time.

To reconstruct the information, now stored in the form of the thickness variation of the thermoplastic, the film is illuminated with a readout laser beam. The phase of this beam will be changed according to the stored thickness variation, which corresponds to a phasehologram.

When heated beyond the melting temperature, the thermoplastic material softens so far, that the stored information is erased. Theoretically, the film could be used after cooling for a next record. This is nevertheless not recommendable due to successive degradation of the thermoplast layer and to possible ghost pictures due to imperfect erasing.

To obtain a homogenous film sensitivity across the whole active aerea, the surface charge has to be perfectly uniform. According to theoretical predictions (11), the sensivity of the film depends at least quadratically on the electric field or the charge density. Usually, the surface has to be charged to several hundreds of volts. The easiest way to do it is by means of a corona discharge in air.

3.3 CAMERA

The camera consists of a mechanical body and of an electronic control unit. The mechanical arrangement and the functions of the camera body are based on the well proven principles and the design as described by R. Moraw (10). We have optimized our camera especially for industrial applications of holographic interferometry. The recording aperture of the camera is 70 x 50 mm. The method we use consists of successive stages of charging, exposure and development.

In the mechanical body, the thermoplastic film is stretched across a carrier plate, made of insulating material. A glass plate with a vacuum deposited, transparent resistive layer on the surface is embeded in the carrier plate in such a way, that the film is guided exactly along its coated surface. The resistive layer on the plate is equipped with contacts in the form of thicker, vacuum deposited conductive strips along two parallel edges of the plate. Two thick copper mesh strips are pressed by rubber cushions against these plate contacts. One of the plate contacts is grounded.

During the sensitizing phase, a carriage with a linear array of needles for corona charging is slowly moved at a constat distance along the film surface. The static charge on the film provides also for its firm adhesion on the glass. For film transport, the carriage lifts the adhereing film from the surface of the glass plate and a motor-winder transports the film.

To assure a perfectly uniform charge distribution on the film surface and thus a uniform sensitivity across the film area, a relatively dense linear array of needles with a precisely defined radius has to be used. We found as an optimum a radius of 0.2 mm and a separation of 2.5 mm. The array has to be somewhat longer then the film width to reduce edge effects. The peaks of the needles have to be adjusted to lie exactly on a straight line. The distance of the peaks to the thermoplastic surface has to be optimized for a given voltage to allow for homogenous charge distribution without any charge concentration in the central part of the film aerea and to prevent local break downs.

Massive breakdowns would damage the transparent resistive layer on the glass, if the output capacitor of the HV power supply could be discharged into the thin layer without a current limitation. To minimize this damage, a HV resistor of several tens of megaohms is inserted into the lead from the HV power supply to the array of needles on the carriage.

After sensitizing, a waiting time of several seconds is necessary before exposure, to allow the mechanical vibrations of the whole camera body to die away.

For development, a current puls is fed to the resistive layer on the glass plate, which acts as a resistive heater and simultaneously as a resistive temperature sensor, allowing to measure the temperature of the heater and to turn off the heating at the appropriate moment. The temperature coefficient of the optically transparent resistive layer (Balzers

Aurell-A3) is nevertheless very low, about +600 ppm/deg C. To measure the turn-off temperature accurately, a high resolution resistance bridge is needed.

Fig.2 shows the simplified circuit diagram of the electronic development control, we use succesfully in our photothermoplastic cameras.

The resistance Rp of the heater builds together with a shunt Rs and the resistors R11, R12, R22 (SW3 open) a Thomson bridge, which eliminates errors due to the resistance of the wiring. The value of Rs is 2 Ohms, the other resistors are kOhm values, being 1000x larger that Rp and Rs. The copper mesh strips are connected on one side to the development-current source, the opposite ends are connected to the bridge circuit.

The bridge circuit, adjusted for balance at Td, is used to detect the achievement of the develop temperature Td and to turn off the heating current. It should be mentioned here, that the develop temperature Td should not be understood as the softening temperature of the thermoplastic material, but rather as the heater temperature at which heating is to be turned off.

With a new heater plate inserted, the bridge has to be prebalanced first, as the heater resistance has a manufacturing tolerance of some +/- 20% around the nominal value of 15 ohms.

A floating voltage source PS2 of a few volts is used to feed the bridge without causing a significant warmup of the heater during the balancing (SW2 closed, SW3 open, T1 nonconducting).

With SW3 open, the bridge is balanced if

$$Rp(Ta)/Rs = R11/R12 = R21/R22$$

where Rp(Ta) stands for the heater resistance at the ambient temperature Ta, at which the bridge was balanced.

The setting of the resistances R11 and R 12 is ganged for proper balancing of the bridge. Each restance is a series combination of low temperature coefficient (15 ppm/deg C) precision resistors, which are switched in steps and of a helipot potentiometer. The precision comparator C (e.g. a uA 734) and a light emitting diode LED serve as a balance indicator.

At the develop temperature Td, the value of Rp will be

$$Rp(Td) = Rp(Ta).\ \{\ 1 + k\ (Td - Ta)\ \}$$

where k stands for the temperature coefficient of the heater layer.

To obtain balance at Td, the value of R12 is decreased (SW3 now closed, potentiometer R112 in parallel to R12) to

$$R12' = R12/\{\ 1 + k\ (Td - Ta)\ \}$$

where R12' is the parallel combination of R12 and R112,

$$R12' = R12xR112\ /\ (R12 + R112)$$

A slight mismatch in the ratio R21/R22 (R22 not being changed correspondingly with R12) decreases marginally the suppression of the wiring resistance; this effect is of no importance, as the resistance change of Rp between Ta and Td is very small.

The correct setting for Td can be hardly calculated, as the necessary temperature overshoot for development depends on many parameters like rate of temperature change, thickness of the film carrier layer etc.. Thus, the setting for Td has to be found experimentally. Once found at any ambient temperature Ta, it keeps valid for any initial conditions of the heater temperature.

The bridge circuitry and the comparator are placed in a sreening box in the camera body. Besides that, the camera body contains a remote controlled HV power supply for the corona charging. All other circuitries are placed in the electronic control unit, which is connected to the camera body by a cable.

From the control unit, only the development-current source is shown in a simplified form in Fig.2. A floating power-supply PS1 charges over a current limiting resistor R1 the electrolytic capacitor C1 = 72,000 uF to 140 volts. A constant-current circuit, consisting of transistor T1, resistor R2 and a Zener diode ZD1 can deliver between 5 to 6 Amps into the heater plate. The current source can be turned on and off by the set-reset flip-flop F-F which controls the optocoupler O.C. and the transistor T2 (both saturated or off). The collector current of T2 feeds the Zener diode ZD1 and turns thus T1 on.

For development, the flipflop F-F is set by a short puls to turn on the heating. The bridge remains unbalanced and

the comparator output high, until Td is reached. Then the comparator restes the flipflop and terminates the heating.

With a constant heating current, the rate of change of the thermoplast temperature is also approximately constant. Obviously, the higher the rate of change of the temperature of the heater, the larger will be the lag in the rise of the temperature of the thermoplast itself, as the heat is transferred from the heater to the thermoplast by conduction through the film carrier and the photoresistive layer. At the moment, when the thermoplast reaches its melting temperature, the heater has already a temperature overshoot due to the mentioned lag and naturally some amount of heat is stored in other components like glass plate etc.. All these overshoot effects can be compensated by a proper setting of the develop (turn-off) temperature Td. With different initial conditions of temperature, the duration of the heating puls will vary, but the develop heat will remain constant.

In the practical circuit, 5 transistors 2N6259 with separate emitor resistors are used in a Darlington stage as T1, to prevent second break-down if a short-circuit across the load should occur. As the capacitor C1 contains only a limited amount of energy, no thermal destruction of the camera could occur even if the electronic switch should fail to open due to some defect in the circuitry. On the other hand, the capacitor must be large enough, to allow to keep the heating current constant until the end of the development, i.e. under typical laboratory conditions between 100 and 400 msec.

The elctronic control unit controls also all other camera functions.

During the sensitizing phase, the film transport and corona charging is controled. The corona voltage Vc can be preset in the range between 5kV and 15kV.

A shutter control allows for a time preset between 50 msec and 5 sec or for a permanent opening of the shutter. For an optimum reproducibility of the holograms, we use an integrating exposuremeter with energy preset for the shutter control (12).

The preset op the develop temperature is done with a helipot potentiometer in the control unit.

After the dry thermal development, a cooling timer with a time preset between 20 sec and 500 sec is started automatically. The fixation of the hologram can be done either by ambient air only, or by forced cooling. In the latter case, a set of fringes may arise due to shrinking effects.

As any running function inhibits automatically a start of any other function, repeated attempts of development in short time intervals, which could damage the plate are also disabled.

We use the same electronics for the large aperture camera of 70 x 50 mm and also for the small aperture camera of 35 x 50 mm. For the small aperture camery only, a capacitor C1 of 24,000 uF is sufficient; only 3 power transistors

are needed as T1 and the heating current can be reduced to 4 to 5 Amps.

3.4. EXPERIMENTAL RESULTS

The experimental results are shown for the use of this thermoplastic film camera in an holographic system. Three tests have been chosen: (1) the transfer characteristics; the diffraction efficiency characteristics; and (3) the spatial frequency response.

Holograms of a diffusely illuminated two-dimensional object were made with approximately 21 deg angle between the object beam and the reference beam R1 and 24 deg for the reference beam R2. The recording and reconstruction wavelengths for all results presented in this paper were 514.5 nm and were recorded with the optical setup shown in Fig.3. In our experiments we used PT 1000S (8) photothermoplastic films with 35 x 50 mm and 70 x 50 mm as recording aperture.

Fig.4 shows the curve of brightness in the reconstructed image as a function of exposure for holograms of a diffused object. The exposure sensitivity of the film is high and comparable to that of high resolution photographic emulsions. We obserd that increasing the potential to which the thermoplastic surface is charged tends to move the curve to lower exposures as predicted theoretically by Gaynor (11). The maximum occurs at an exposure of about 0.8 uJ/cm sq.

The most critical factor at the development stage is the thermoplastic develop heat. As mentioned above, this heat is determined primarily by the rate of change of temperature during the heating and by the develop temperature Td, at which the heating is turned off. This turn-off temperature is always higher than the melting temperature of the thermoplastic, as the melting heat has to be delivered to the thermoplastic in a very short time during this tem perature overshoot. With different initial conditions of temperature, the duration of the heating pulse will vary, but the develop heat will remain constant.

The dependence of the brightness of the reconstructed image on the develop temperature is given in Figs.5 and 6. These results, especially the one in Fig.5, show clearly that the reproducibility in the brightness of the reconstructed image of thermoplastic holograms depends very strongly on the develop heat and thus also on the develop temperature Td. On the other hand, the Fig.6 shows, that the duration of the heating puls has no significant influence on the brightness, as expected. A deviation of +/-0.5 deg C from the optmum develop temperature results typically in a decrease of the brightness of the reconstructed image by 25%.

Te constant-current heating controled by a direct measurement of temperature allos to keep the develop temperature and thus also the develop heat reproducibly within a narrow limit independent of ambient temperature variations or

undefined initial thermal conditions of the heater at repetition rates with intervals below 5 minutes. This results in only +/- 5% variation in brightness of the reconstructed image.

The specially designed corona geometry allows to improve the homogeneity of the efficiency over the recording frame. We have experimentaly found that the variation of the efficiency over the recording area (70 x 50 mm) is about +/- 2%.

In order to measure the signal-to-noise ratio (SNR), we utilized as the object a white painted surface whose central part was covered with an opaque strip. The SNR was determined by scanning the reconstructed real image with a pinhole-photomultiplier tube assembly and by computing the ratio of the averaged intensities across the illuminated and the opaque part of the image. The result is given in Fig.4 and is obtained at a spatial frequency of 650 L/mm with the corona voltage Vc of 14.5 kV and a reference-to-signal beam ratio of 1. In Fig.7 the brightness in the reconstructed image at a spatial frequency of 650 L/mm is shown as a function of the beam ratio. The maximal brightness in the reconstructed image is not coincident with the highest SNR.

To determine the diffraction efficiency we recorded holograms with a setup shown in Fig.3. Diffraction efficiency is the percentage of the incident light diffracted into the first order by the hologram. The maximum diffraction

efficiency we achieved with PT 1000S for a diffused object was about 30% at a spatial frequency of 600 L/mm as it is shown in Fig.8.

In our holographic experiments with the PT 1000 type thermoplastic film we obtained for a diffuse object a bandpass response for spatial frequencies with a maximum at 550 L/mm and a useful range from 350 to about 900 L/mm as shown in Fig.9, shere Io*(NORM) is the distribution of the brightness in the reconstructed image divided by the light distribution of the illuminated object. For these measurements, the same pinhole-photomultiplier tube assembly is used. Short exposure times lead to additional suppresion of the higher frequencies. The knowledge of this response allows to estimate the maximum size of a recordable object as well as to design a special object illumination which compensates for the intensity losses at higher frequencies.

3.5. CONCLUSIONS

The thermoplastic recording medium has a considerable potential for many holographic applications. It offers ease and convenience to the rapid in situ process of recording and reconstructing of large aperture holograms.

The panchromatic and sensitive photoconductor gives the medium a response comparable to that of high resolution photographic emulsions. Furthermore, the thermoplastic dorms relatively efficient thin phase holograms. The

holograms can be formed over a broad range of exposures, but are much more sensitive to the develop heat. Although the sensitivity to the develop step is an inconvenience, it is relatively straightforward to use the constant-current resistive heating and a direct measurement of the heater temperature for an accurate develop heat control. Finally the addition of a special designed corona geometry permits rapid and uniform charging.

The investigations show that the performance of a thermoplastic film camery can be optimized to such an extend that even difficult holographic recordings with large appertures, e.g. as needed for industrial applications of dual reference-beam holography (14) and heterodyne holography (15), can be made in a routine manner.

4. FRINGE COUNTING

It is instructive to compare heterodyne interferometry and classical fringe counting interferometry with the help of Fig.10, which shows the interference phase $\phi(\vec{x})$ as a function of the position x in an arbitrary direction across the fringe pattern. The position xi of the dark and bright fringes are determined by the maxima and minima of the cosinefunction. This means $\phi i = m$ for the corresponding values of the interference phase, where m is an integer. Therefore only a limited number of samples of

$\phi(\vec{x})$, equi-distant in phase rather than in space, can be obtained. The accuracy of the determined fringe positions xi depends strongly on the slope of $\phi(\vec{x})$ and on the resolution of the intensity detection within the fringe pattern, because of the fact that the intensity is stationary at the maxima and minima of the cosine-function. Interpolation between the fringes is not very reliable since any intermediate value of the intensity in the fringe pattern depends both on phase and average intensity, which is in general not constant across the image.

The heterodyne interferometry overcomes this limitation, because phase and amplitude of the interference term can be separated electronically and the fringes travel across the image so that the sensitivity and accuracy is the same at any position. As indicated in Fig.10 one may select any arbitrary position xn or even a set of equidistant positions, and determine the corresponding value ϕ n of the interference phase.

5. VIBRATION ANALYSIS

Holographic interferometry, applied to the determination of body motion, has been demonstrated by a number of investigators (16,17). Time-average holographic interferometry of sinusoidally vibrating object has been investigated by Powell and Stetson (18).

In real time holographic interferometry only one wave field has to be stored holographically, therefore there is no need for two-reference-beam recording. In this case the frequency offset has to be introduced between the reconstructing reference beam R1 and the object illumination, as shown in Fig.11. Two possible setups with acousto-optical moldulators are sketched in Fig.12. The two modulators can be either placed in cascade in the reference beam, or one in the reference beam and the other one in the object illuminating beam, similar as shown in Fig.11. The modulators are driven at identical frequencies $\Omega 1 = \Omega 2$ for the hologram recording and at different frequencies $\Omega = \Omega 1 - \Omega 2$ for the heterodyne evaluation. The interference phase measurement is expected to be less accurate than in the case of double exposure heterodyne holographic interferometry, since the object wave fields show considerable phase variations. The accuracy of the phase measurements depends besides the electronic equipment essentially on the mechanical stability of the optical setup and the amount of statistical phase fluctuations due to air turbulence in the optical paths. But the real-time arrangement has the advantage that the temporal behavior of the interference phase $\phi(t)$ can be determined quantitatively for a fixed point or with additional detectors at several points simultaneously. The temporal resolution is limited by the integration time of the phasemeter and finally by the difference frequency employed. From

phasemeter with an analog output one gets a direct, continuous display of the time dependent interference phase either on an oscilloscope or on a plotter.

Real-time heterodyne holography allows to investigate the temporal behavior of vibrations, but only at one or a few points simultaneously, depending on the number of detectorts employed.

Time-average holography, which is most commonly used for holographic vibration analysis, can not be combined with heterodyne evaluation, since the interference fringes are already frozen in the hologram.

The use the full potential of accuracy, heterodyne holographic interferometry it is therefore necessary to store the information of the vibration amplitude holographically by some kind of double exposure recording and to perform the evaluation under stationary conditions afterwards. This can be accomplished by combination of stroboscopy and two-reference-beam holography. A corresponding setup, using three acousto-optical modulators, is sketched in Fig.11. Each of the two reference beams R1 and R2, as well as the object illuminating beam pass through one of the modulators, which are adjusted to give maximum output in the first order diffracted beam. During recording they are driven at identical frequencies $\Omega 1 = \Omega 2 = \Omega 3$ and used as amplitude modulators or fast shutter to generate the stroboscopic illumination.

During reconstruction only the reference waves are used and their modulators are driven at slightly different frequencies 1 and 2 to generate the difference frequency for the heterodyne detection in a similar manner as described earlier in this paper. The puls trains of the driving power fed to the three modulators are shown in Fig.13, together with the vibration amplitude, which has to be detected at one point of the object for synchronization purpose. The object is illuminated during an appropriate time in its two extreme positions of positive and negative vibration amplitude (19). The reference beams R1 and R2 are alternatively switched on at the same intervalls, so that one reference beam records only the positive and the other one only the negative extreme position of the vibration. The result of this type of stroboscopic recording is a two-reference-beam hologram with independent recording of the two extreme positions of the vibrating object. The reconstruction of such a recorded hologram is shown in Fig.6 Standart acousto-optical modulators at 40 Mhz driving frequency can be used straightforward as amplitude modulators or fast shutters with pulse durations down to 1 us or even shorter. Such a recorded hologram can be evaluated by the heterodyne method in the same manner and with the same accuracy as described earlier in this paper for dual reference beam holograms. Fig.15 shows the reconstructed stroboscopic two-reference-beam hologram of a moving turbine blade where the optical phase of the reference beam R2 is

shifted. In comparison to the reconstruction in Fig.14 the interference fringes are at a given point just 180 deg in phase apart.

6. ELECTROMAGNETIC FORCING DEVICE

For a contact-free excitation of vibrations of objects made from ferromagnetic materials an electromagnetic forcing device was developed.

A U-shaped electromagnet with a crossection aerea S of the magnetic core and a current I flowing through its N-windings is placed at a distance D from the surface of the object to be excited. As known, the force F exhibited by the electromagnet on the object is

$$F = \frac{1}{2} I^2 \frac{dL}{dD} = -\mu_o (NI)^2 \frac{S}{4D^2}$$

For a vibration amplitude negligibly small agains the distance D, the force is

$$F = \text{const. } I^2$$

Due to the square-law, a direct excitation with a sine-wave current would lead not only to a frequency doubling, but also to a variable dc bias force, which would be dependent on the amplitude of the excitation current. This would cause severe troubles e.g. for double exposure holograms, where the original (nonvibrating) state is compared with the excited state, as a tilt-bias would be superimposed on the vibration pattern.

To avoid this trouble, a dc bias current is applied to the electromagnet and an ac current component is superimposed in such a way, that the sum of both currents never reaches zero.

To obtain a sine-wave force response for a sine-wave input signal, the current, feeding the coil is generated in the electronic circuitry to obey to the square-root lwa, namely

$$i(t) = k' \cdot (1 + m \cdot \sin \omega t)^{1/2}$$

resulting then in a force of

$$F(t) = F_o \ (1 + m \cdot \sin \omega t)$$

Fig.16 shows the electronic circuitry, which generates the coil-driving current. A dc bias is added to the ac input signal. An operational amplifier with a squarer (Burr-Brown 4302) in the feedback build the square-root of the sum of both signals. The square-root signal is the input to an output power amplifier, consisting of a Darlington transistor and current feedback loop with an additional operational amplifier. The current range and thus also the range of achievable force can be adjusted by the emitor resistor of the output Darlington. The frequency range for maximum force is limited primarily by the inductance of the excitation-coil and the supply voltage for the output stage.

An additional electronic circuitry, not shown in the block-circuit diagram checks the signal levels in the electronics for possible overloads. The input signal to the squarer is checked to be positive within about 1 to 9 Volts limit, the

collector voltage of the output Darlington is checked for saturation. Any of these overloads would namely case a considerable harmonic distortion of force.

The electromagnet itself is made of a laminated U-shaped transformer core of about 1 cmsq crossection aerea. About 100 turns of aluminium wire are wound symmetrically on both straight parts of the U. For fastening of the electro-magnet, a screwed clamping device squeezes the round part of the U.

The clamping device is crewed to a piezo force-gage (Wilcoxon Research, Model L10), which serves for direct force monitoring. Finally, the force gage is fixed to a large mass (brass cylinder of about 15 kg).

To damp the mechanical resonances of the system, sheets of acoustic damping material (Antiphone) are placed between the piezo-gage and the brass cylinder. Besides that, the whole electromagnet assembly is damped with this material. It fills the inside of the U (beeing squeezed between the both haves of the winding) and is further wound around the outside of the wire-windings and squeezed to the surface by a metal strip.

A charge amplifier is placed near to the piezo-gage; it's output serves for direct monitoring of the force.

With this electromagnet, the resonance of the monitor system is about 8 kHz, the maximum force with D=0.5 mm

about 1 Newton. The force response as such is practically flat up to 8 kHz, monitoring is useful up to 5 KHz (low-pass filter cascaded to the output of the charge amplifier to suppress the resonance peak of the monitor).

The full-force (1 N) frequency range is limited by the 24 Volts supply voltage for the power amplifier to about 5 kHz. The dc bias current for the electromagnet is 1 A.

A slight harmonic distortion of the force is due to various uncontroled nonlinearities in the system. For D=0.5 mm to 2 mm, the harmonic of the force are

2nd: more than -30 dB below fundamental (30 Hz to 2 kHz)
more than -20 dB " " (2 kHz to 6 kHz)
3rd: -50 dB to -35 dB " " (30 Hz to 6 kHz)

Higher harmonic fall all below these limits.

For force colibration, frequency response measurements and harmonic distortion measurements, another Wilcoxon piezo gage of the same type was used. A relatively light iron bar was attached to it's surface, the piezo gage was fixed in a heavy bench vice. The own resonance of this system was about 22 kHz. The U-shaped electromagnet was placed to exhibit it's force on the iron bar. For measurements, the hp 3582A spectrum analyzer was used.

7. STROBOSCOPE

Acousto-optical modulators (Bragg-Cells) are used as fast shutters for stroboscopy. For each beam a Bragg-Cell is needed. Without acoustic field, the laster beam passes the Bragg-Cell without any change in direction and is blocked off by a stop. With an acoustic field applied, the beam is deflected by the Bragg-angle and passes along the stop.

Thus, to produce the stroboscopic pulses, the Bragg-Cells have to be fed with high frequency puls bursts, the timing of which corresponds to the desired illumination pulses P1, P2 and P3 as shown in Fig.13.

The Bragg-Cell type used (IntraAction Corp. AOM-40) requires an input power of about 2 Watts into 50 Ohms, the operating frequency is 40 MHz. Each of the cells is driven by a separate hf power amplifier (ENI 300P or similar). A 40 MHz quarz oscillator is used as the high frequency signal source.

Fast transmission gates are connected between the signal source and each input of the rf power amplifiers. The gates are controlled by puls signals as shown in Fig.13. The gates are of the 6-diode type, use Schottky diodes and are controlled by Schottky TTL logics. The turn-off attenuation is better than 60 dB.

The strobing pulses P1, P2 and P3 have to be generated synchronously with the vibration excitation or detected

vibration. An analog computing circuit measures the duration of the vibration period and computes for the strobing pulses the delay from the zero crossings of the vibration signal and the width of the strobing pulses. Both, the delay and the width of the strobing pulses can be separately preset in percentage of the period time; this preset is thus independent of the vibration frequency.

8. MEASUREMENT OF MECHANICAL STRAIN AND STRESSES

Holographic interferometry applied to dynamic deformations of solid objects generates in general fringes which are contour lines of the surface displacement in the direction of the sensitivety vector. In many practical applications, however, it is rather the differential change of the surface displacement, than the displacement itself, which is of primary interest. The surface strain is essentially related to the local derivatives of the fringe pattern. Obviously heterodyne holographic interferometry is a powerful tool to determine local derivatives of the interference phase, thanks to its capability of accurate fringe interpolation. Therefore straight forward numerical differentation of the measured interference phase can be used to calculate strain and stresses.

9. CONCLUSIONS

It has been shown and experimentally verified that stroboscopic, two-reference-beam heterodyne holographic interferometry can be applied to vibration analysis. Moreover, real time holographic interferometry is suitable for vibration studies with an upper limit given by the frequency offset Ω; however the overall stability has not yet been verified experimentally.

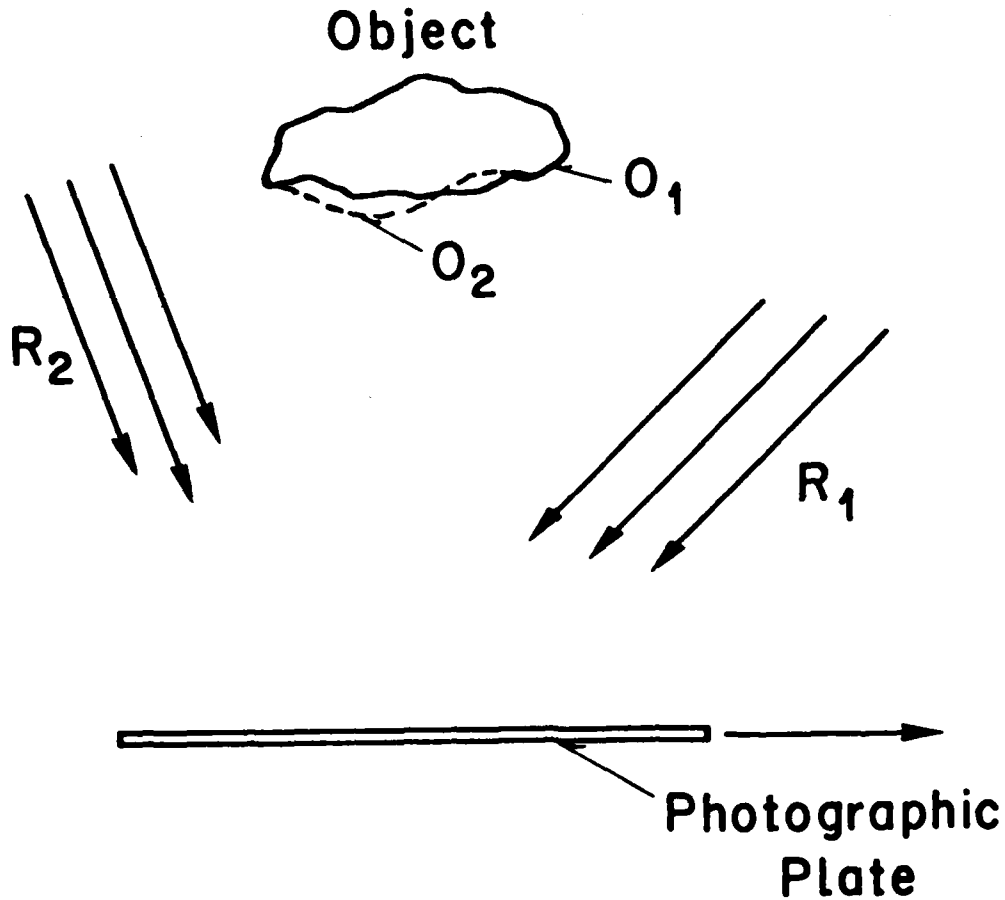

Fig. 1: Setup for recording double exposure holograms with two reference beams.

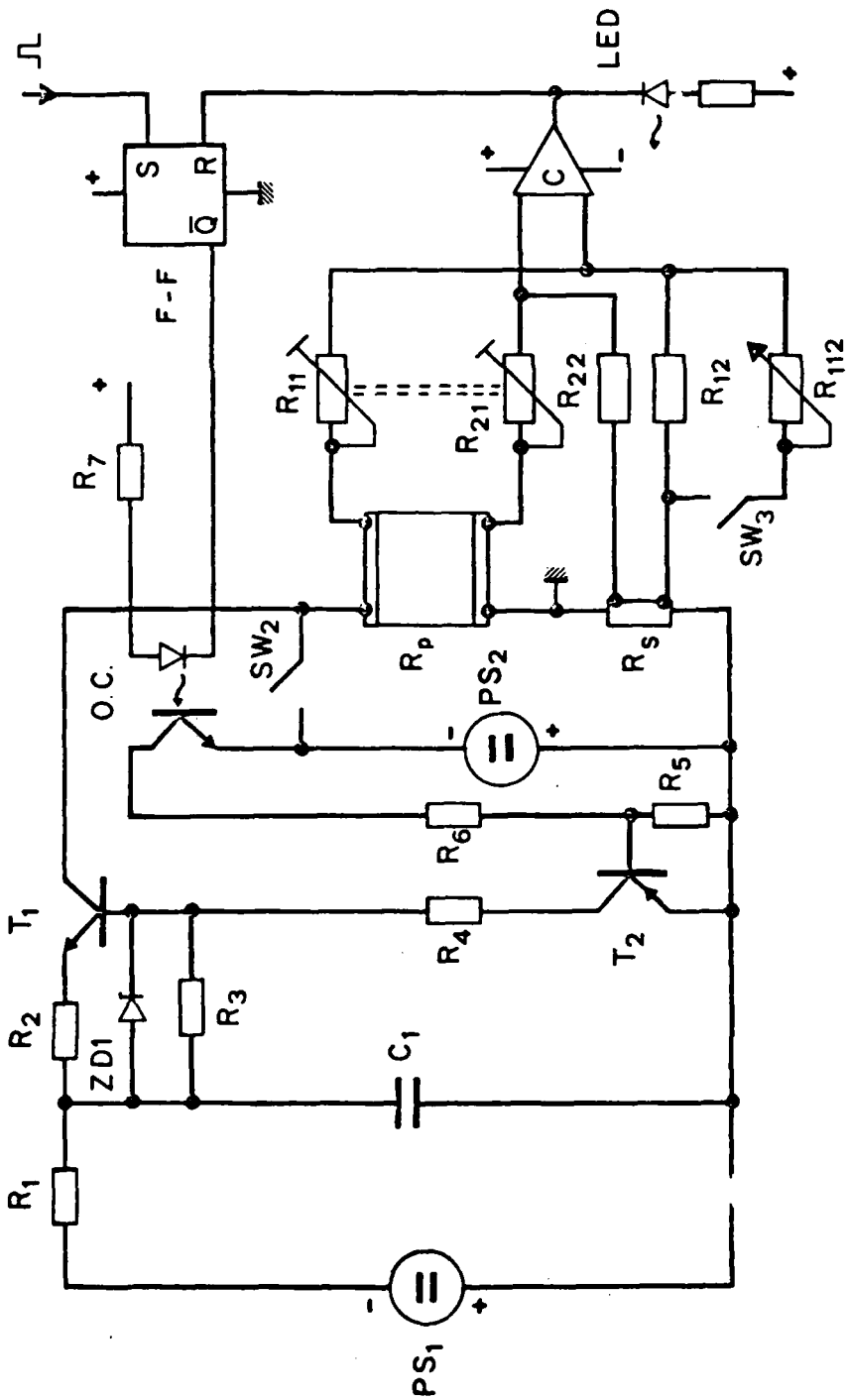

Fig. 2: Simplified circuit diagram of the development control

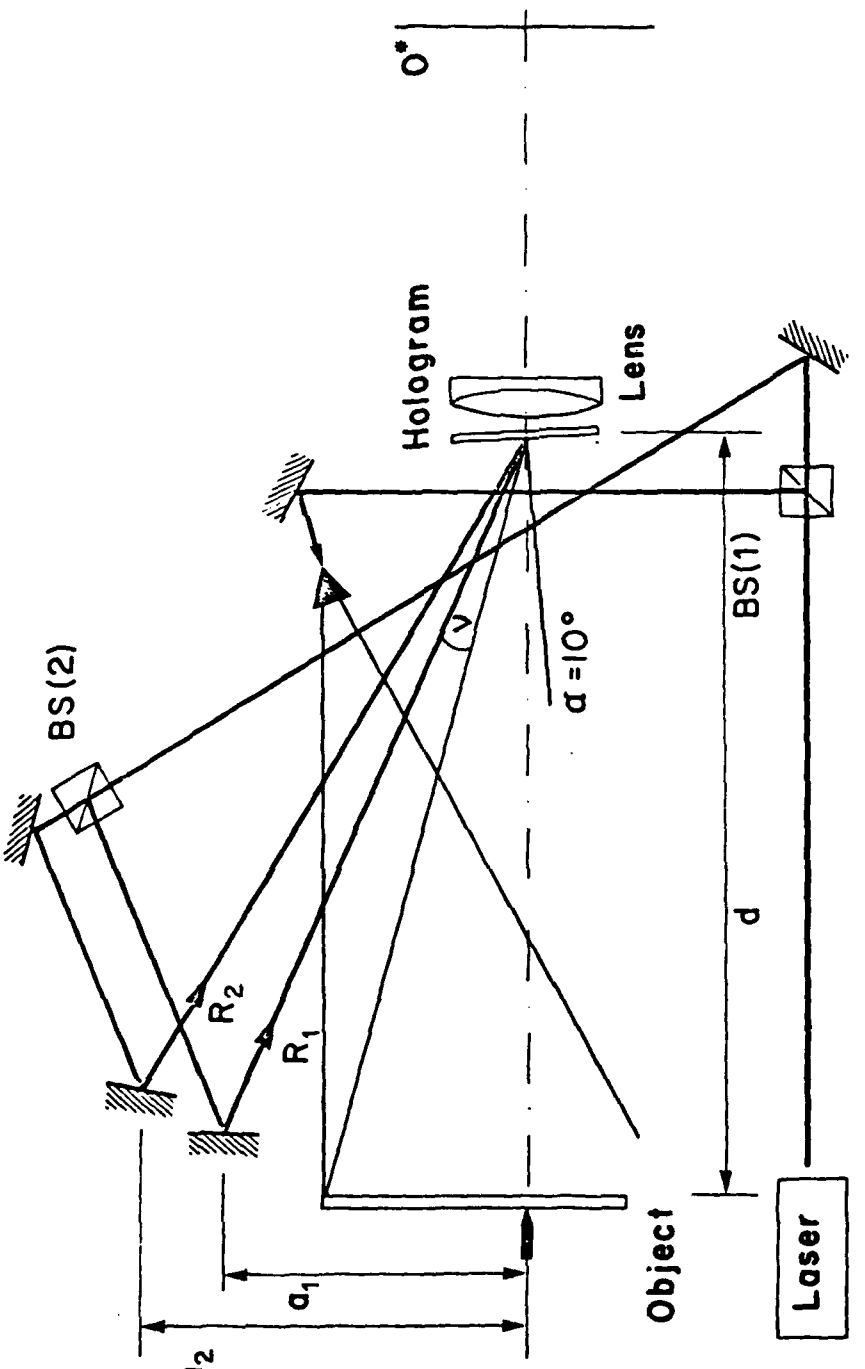

Fig. 3: Holographic setup for the measurements of transfer characteristics, diffraction efficiency and spatial frequency response.

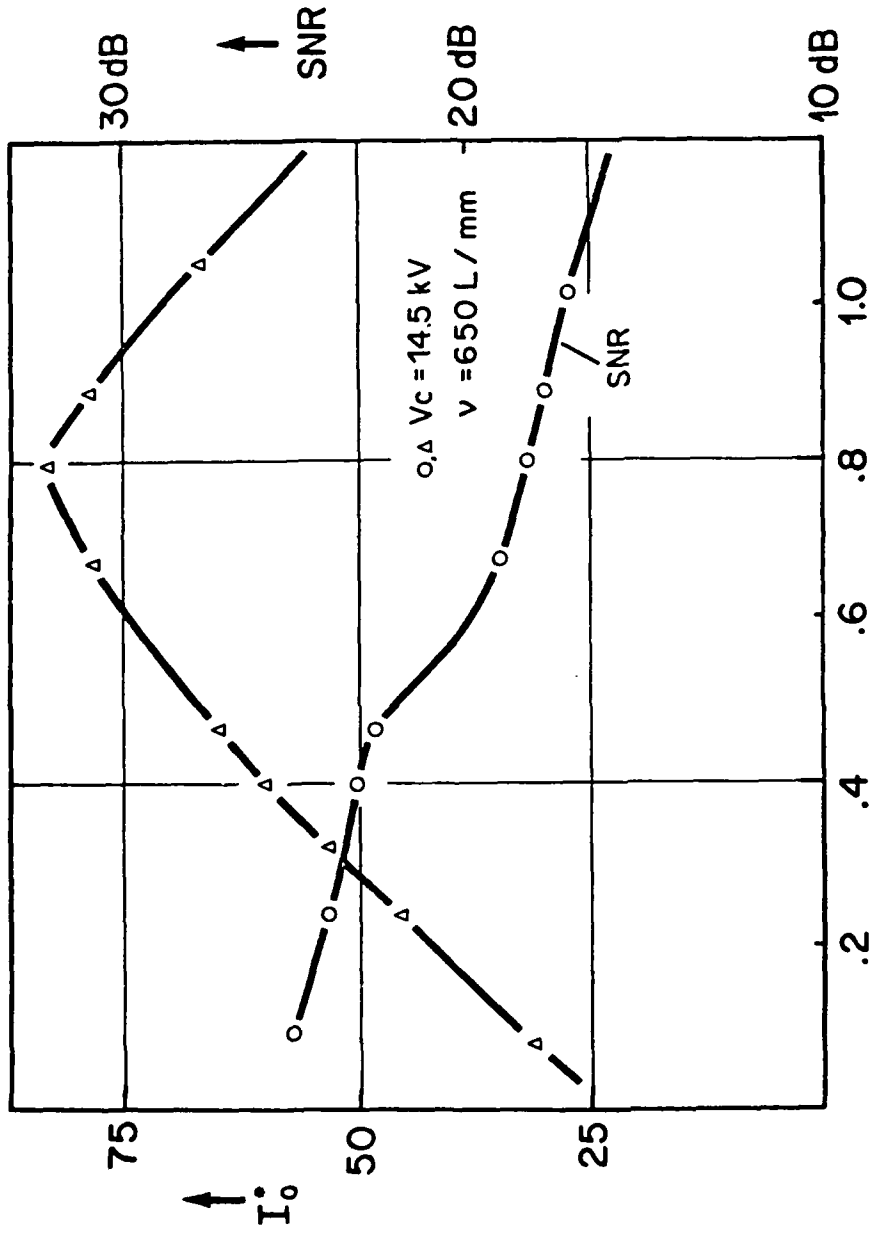

Fig. 4: Curve of brightness and SNR in the reconstructed image of thermoplastic holograms as a function of exposure energy.

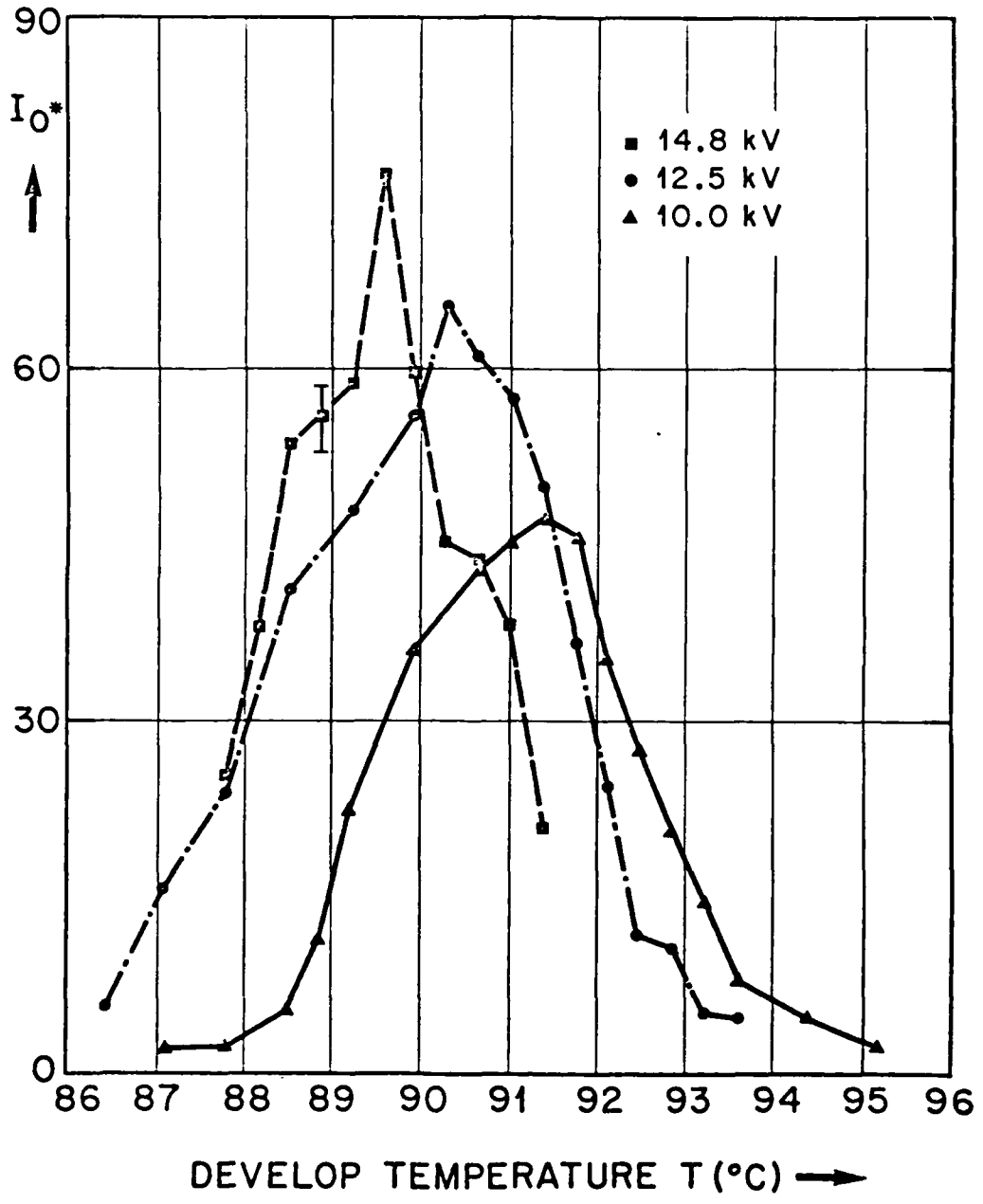

Fig. 5: Experimental result showing the brightness in the reconstructed image vs develop temperature for different corona voltages Vc.

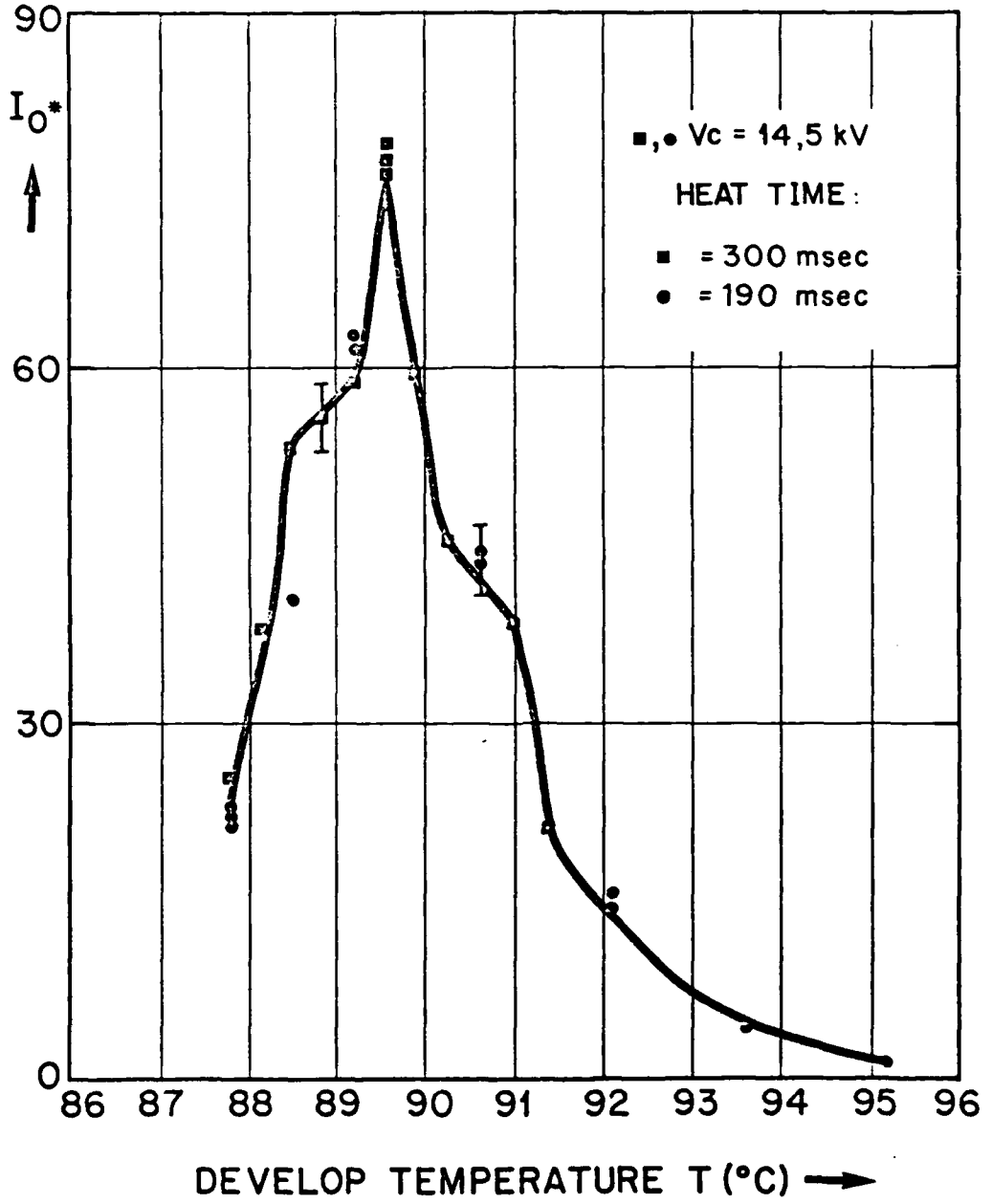

Fig. 6: Representative curve for develop temperature and different heating times.

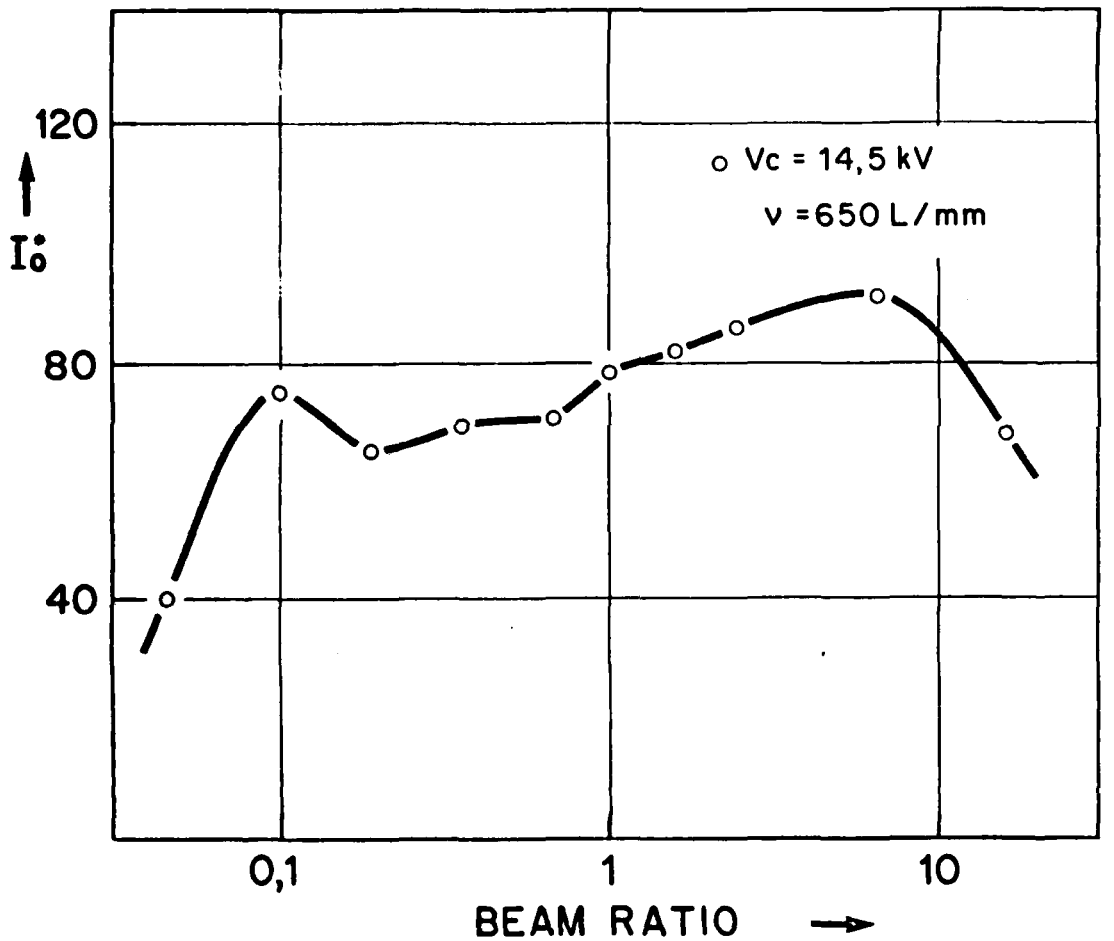

Fig. 7: Brightness in the reconstructed image vs reference-to-signal beam ratio.

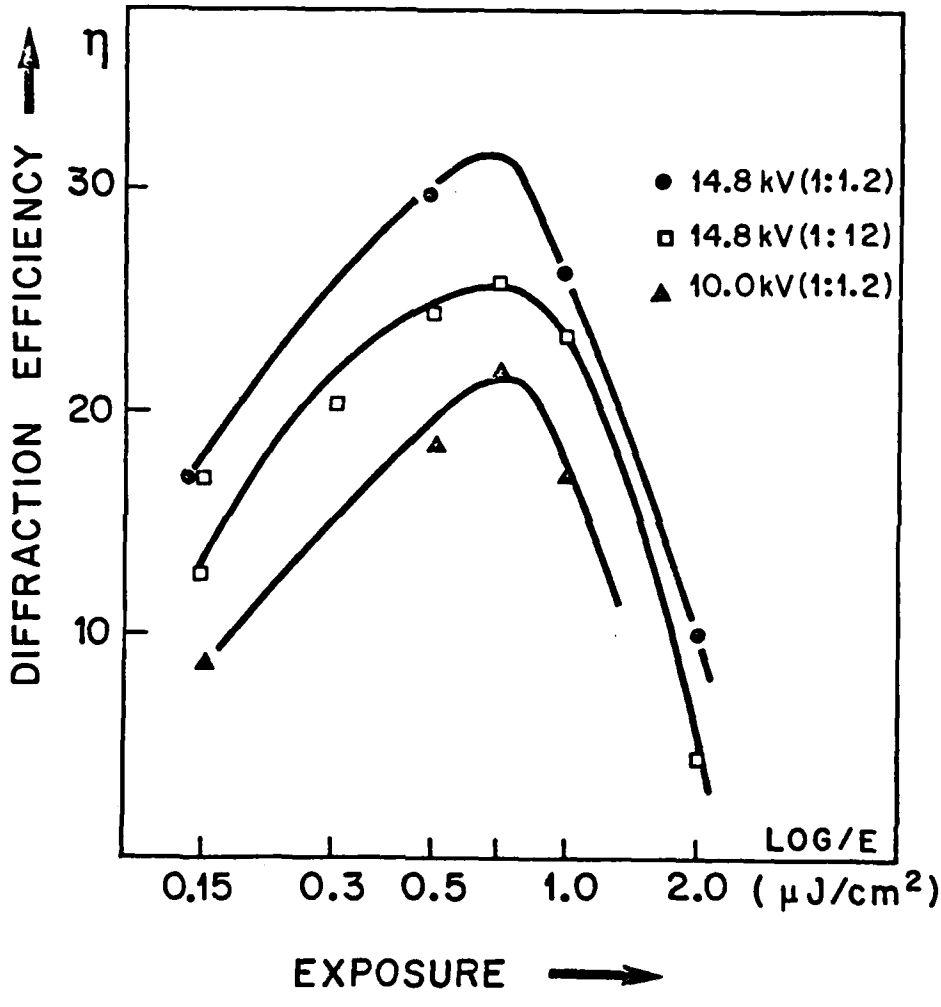

Fig. 8: Graph showing the dependence of diffraction efficiency on exposure.

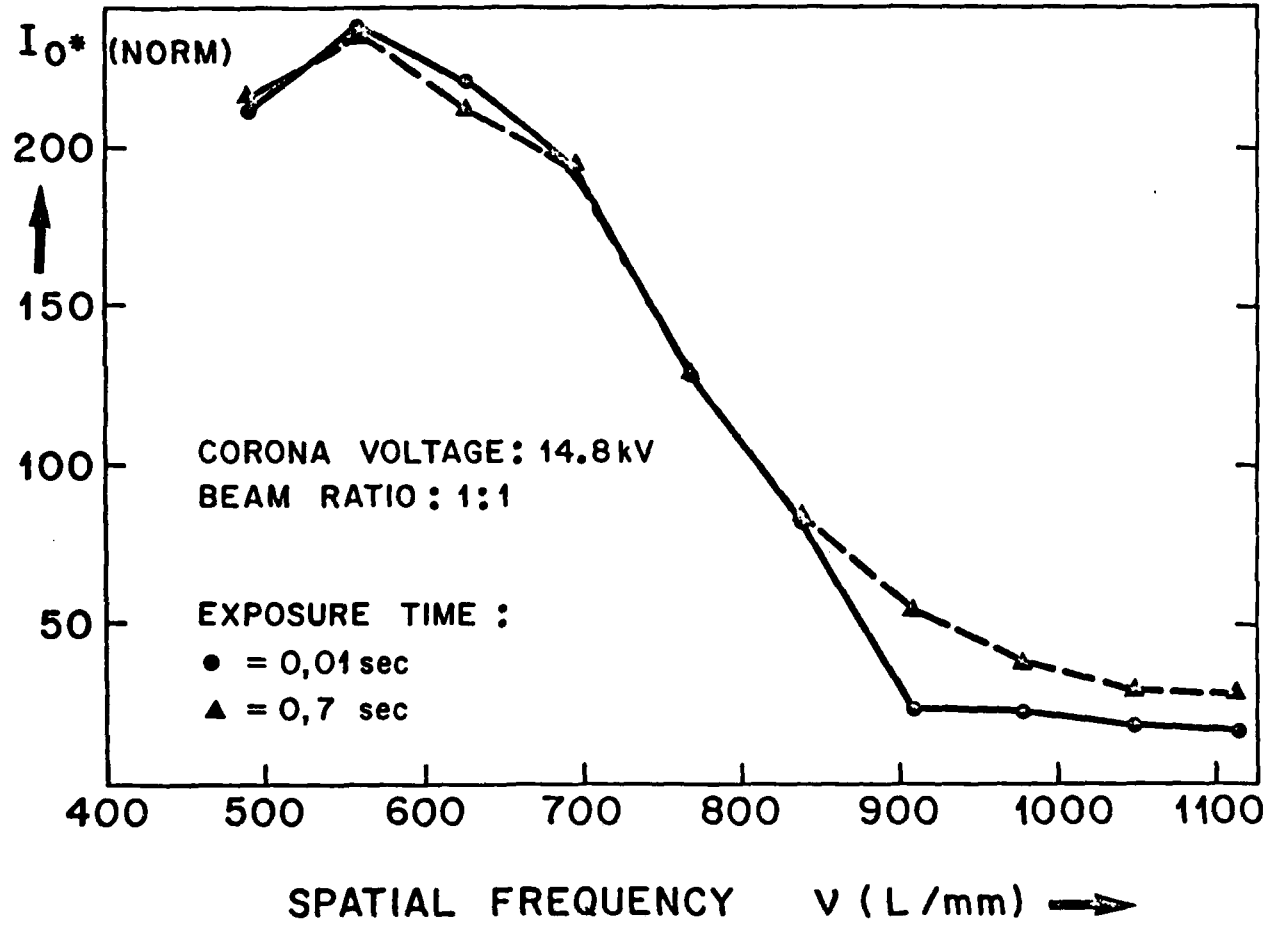

Fig. 9: Dependence of brightness in the reconstructed image on spatial frequency with different exposure times.

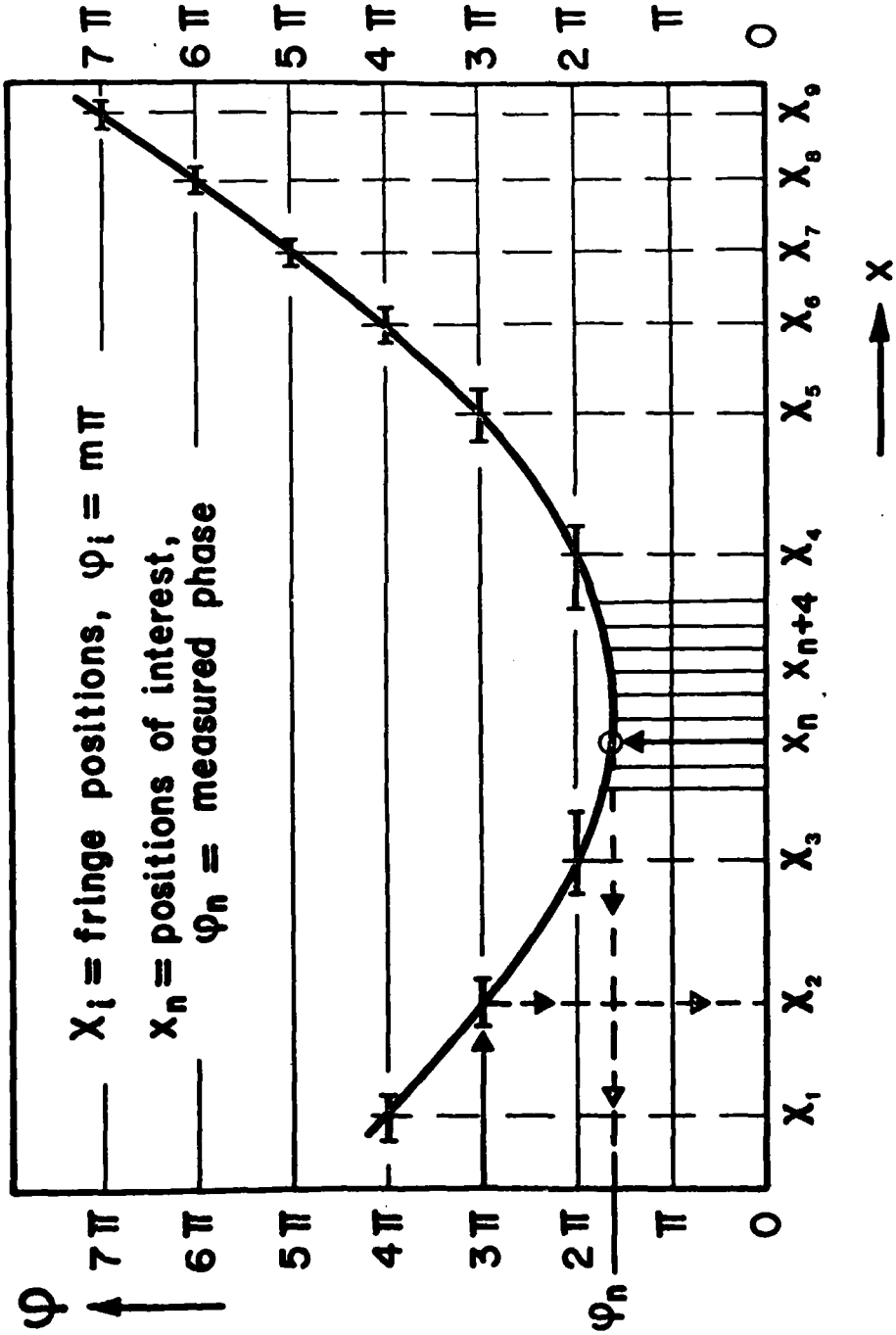

Fig. 10 Comparison of fringe counting and interference phase measurement.

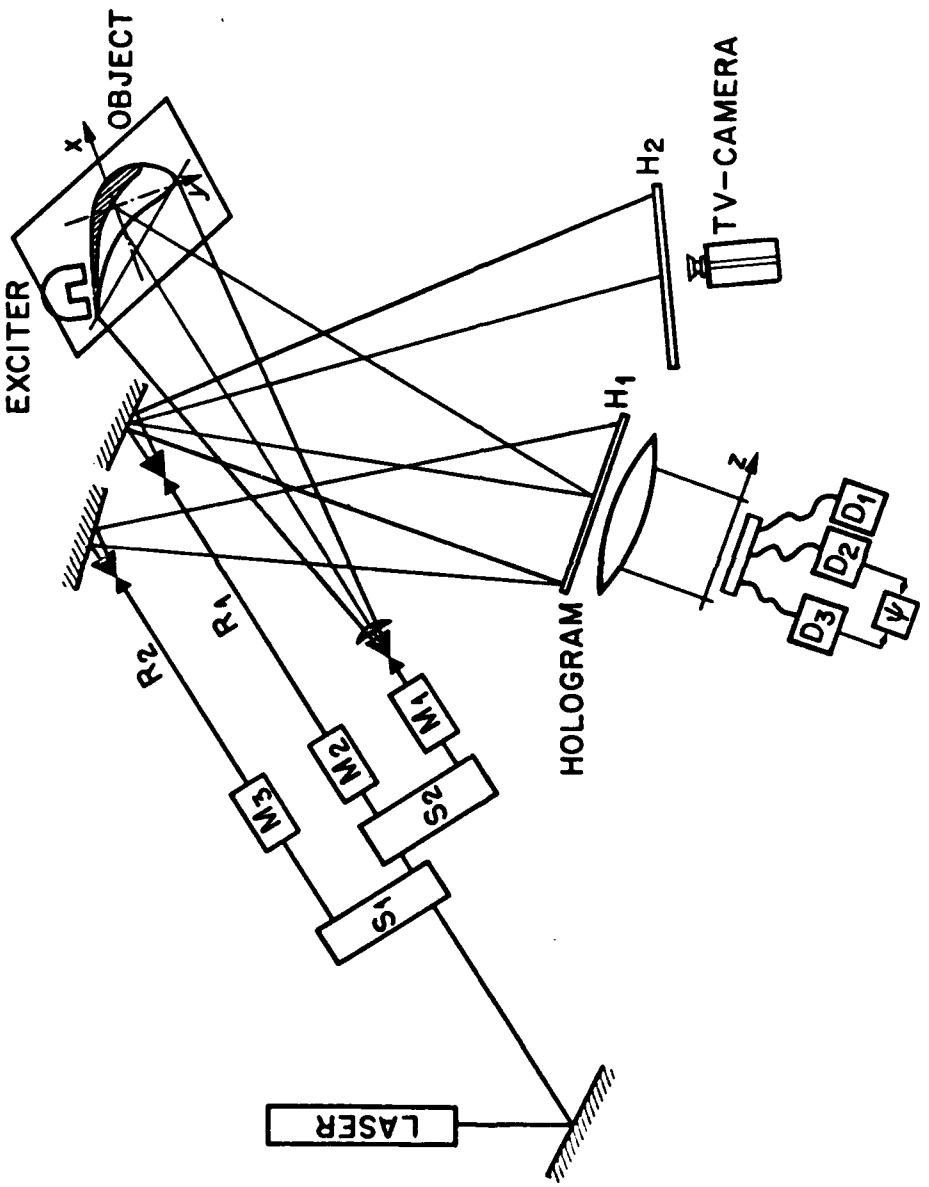

Fig. 11: Experimental setup for two-reference beam heterodyne holographic interferometry and real-time heterodyne evaluation.

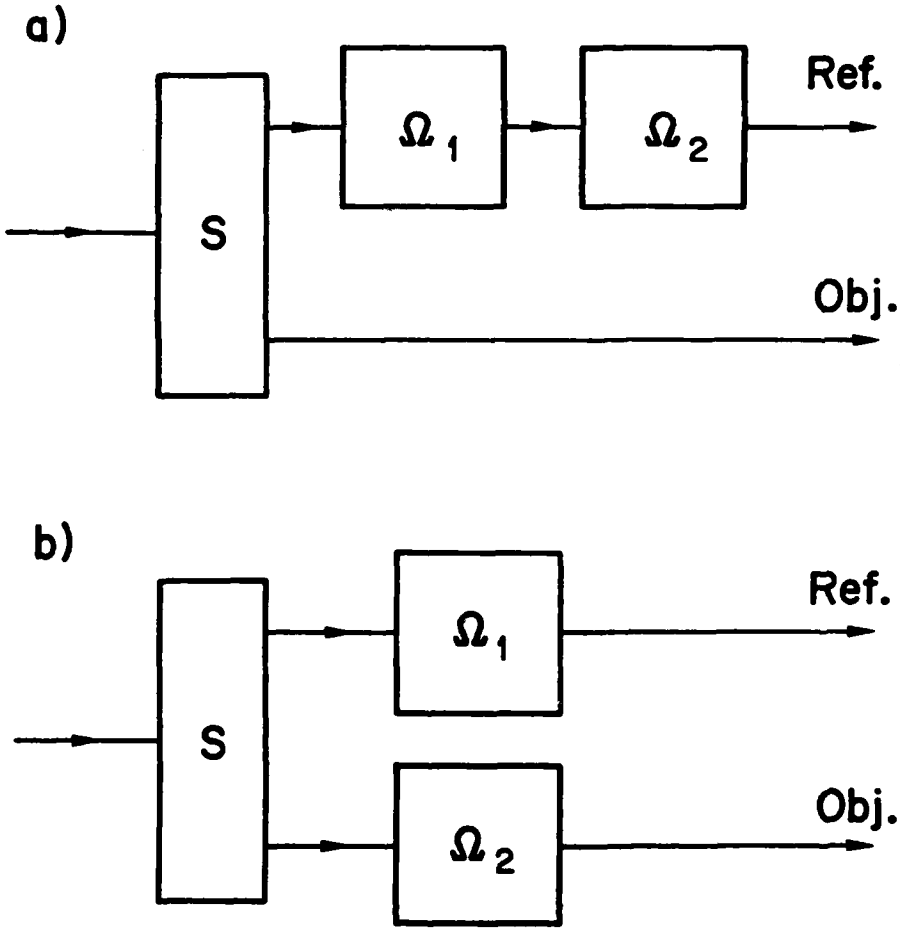

Fig. 12: Arrangement for the two acousto-optical modulators.

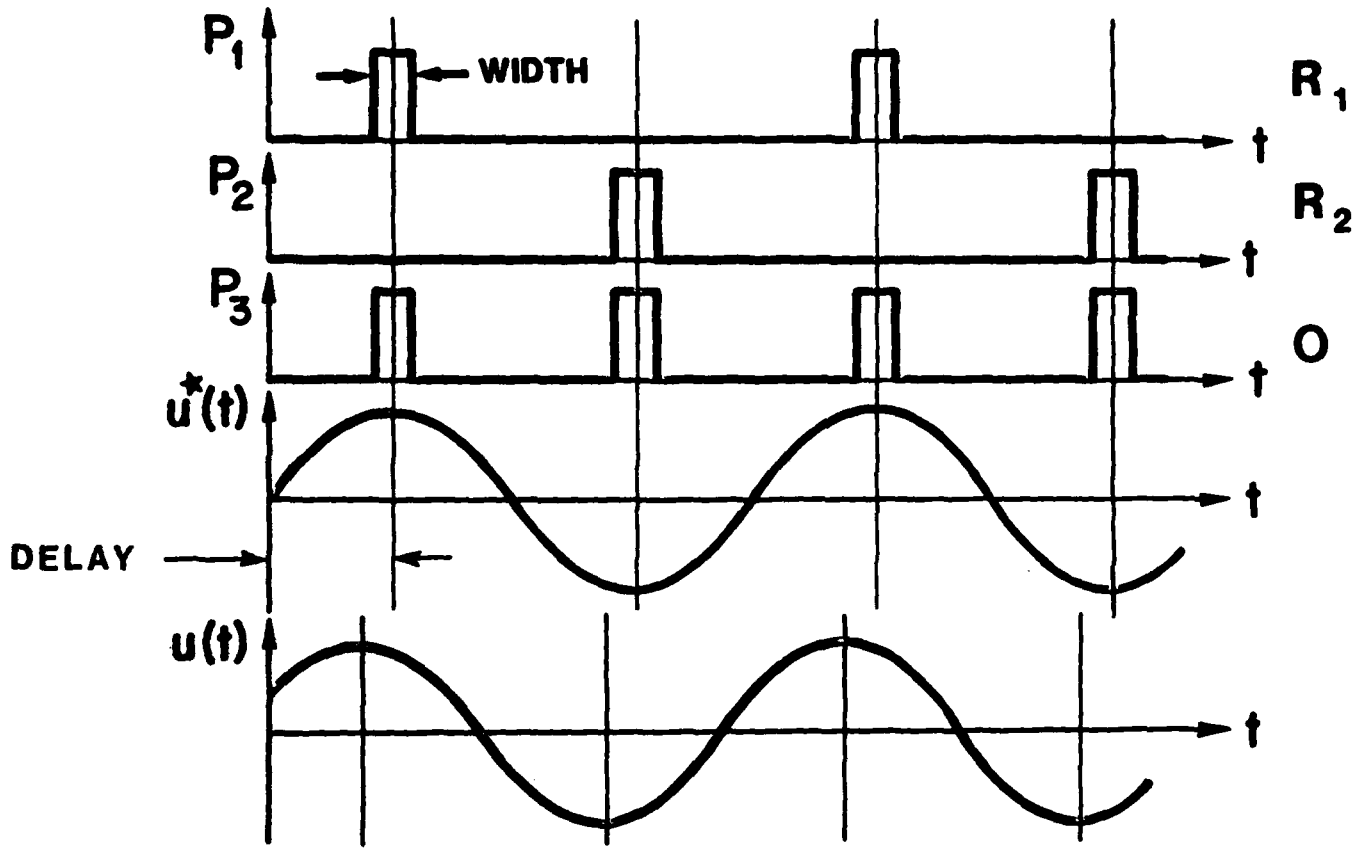

Fig. 13: Exciting amplitude, vibration amplitude and corresponding rf-power pulses P1, P2, P3 applied to the modulators M1, M2, M3 to record a stroboscopic two-reference-beam hologram.

Fig.14: Reconstruction of a multiple exposure hologram of a vibrating object with stroboscopic illumination.

Fig. 15: Reconstruction of the same hologram as shown in Fig.6 but with $\lambda/2$ shift of one reference beam.

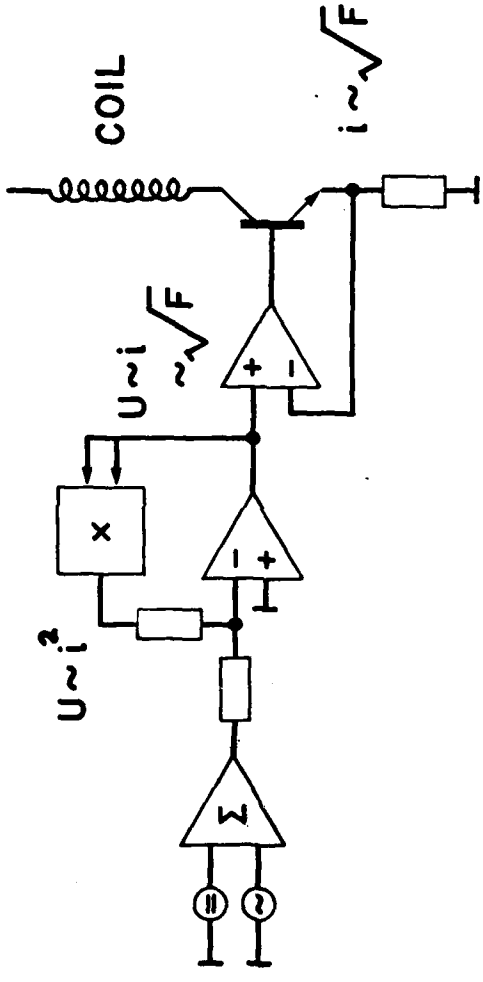

Fig. 16: Simplified circuit diagram of the electromagnetic forcing device.

REFERENCES

(1) R. Daendliker, E. Marom, F.M. Mottier, J. Opt. Soc. Am. 66, 23 (1976)

(2) R. Crane, Appl. Optics, 8, 538 (1969)

(3) M.J. Dentino, C.W. Barnes, J. Opt. Soc. Am. 60, 420 (1970)

(4) R. Daendliker, B. Ineichen, F.M. Mottier, Opt. Commun. 9, 412 (1973)

(5) J. Mastner, V. Masek, Rev. Sci. Instr., 51, 926 (1980)

(6) Di Chen, J.D. Zook, Proc. IEEE 63, 1207 (1975)

(7) G.W. Stroke, Opt. Acta 16, 401 (1969)

(8) R.K. Erf, *Holographic Nondestructive Testing* (Academic Press, New York, 1974)

(9) W.E. Glenn, J. Appl. Phys. 30, 1870 (1959)

(10) R. Moraw, Proceedings of The Laser 75 Optoelectronics Conference, 179 (1975)

(11) J. Gaynor, S. Aftergut, Phot. Sci. Eng. 7, 209 (1963)

(12) V. Masek: (to be published)

(13) R.T. Pitlak, Electro-optical Syst. Design, 6, 46 (1978)

(14) R. Daendliker, E. Marom, F.M. Mottier, J. Opt. Soc. Am 66, 23 (1976)

(15) R. Daendliker, B. Ineichen, F.M. Mottier, Opt. Commun. 9, 412 (1973)

(16) R.J. Collier, E.T. Doherty, and K.S. Pennington, Appl. Phys. Letters 7, 223 (1965)

(17) R.E. Brooks, L.O. Heflinger, and R.F. Wuerker, Appl. Phys. Letters 7, 248 (1965)

(18) R.L. Powell, K.A. Stetson, J. Opt., Soc. Am. 55, 1593 (1965)

(19) C.C. Aleksoff in Holographic Nondestructive Testing, ed. R.K. Erf (Academic Press, New York) 247 (1974)

END

DATE
FILMED

5 83

DTIC